

Deepened Graph Auto-Encoders Help Stabilize and Enhance Link Prediction

Xinxing Wu
University of Kentucky
Lexington, Kentucky, United States

Qiang Cheng*
University of Kentucky
Lexington, Kentucky, United States

Abstract

Graph neural networks have been used for a variety of learning tasks, such as link prediction, node classification, and node clustering. Among them, link prediction is a relatively under-studied graph learning task, with current state-of-the-art models based on one- or two-layer of shallow graph auto-encoder (GAE) architectures. In this paper, we focus on addressing a limitation of current methods for link prediction, which can only use shallow GAEs and variational GAEs, and creating effective methods to deepen (variational) GAE architectures to achieve stable and competitive performance. Our proposed methods innovatively incorporate standard auto-encoders (AEs) into the architectures of GAEs, where standard AEs are leveraged to learn essential, low-dimensional representations via seamlessly integrating the adjacency information and node features, while GAEs further build multi-scaled low-dimensional representations via residual connections to learn a compact overall embedding for link prediction. Empirically, extensive experiments on various benchmarking datasets verify the effectiveness of our methods and demonstrate the competitive performance of our deepened graph models for link prediction. Theoretically, we prove that our deep extensions inclusively express multiple polynomial filters with different orders.

1. Introduction

The rapid advances [3, 11, 18, 19] in deep neural networks (DNNs) have generated widespread impacts to many fields, including natural language understanding, speech recognition, image classification, and video processing. In general, DNNs are quite effective in dealing with regular or Euclidean data, but they become ineffective for irregular or non-Euclidean data, such as the citations of papers in the academic publication [32], the hyperlinks of web pages on the world wide web [25], and so on. These data, typi-

cally irregular, complex, and of considerable dependencies, are often described in the form of graphs, posing notable difficulties to popular neural network algorithms for regular or Euclidean data. In order to model the interrelationship and structures of these data, graph neural networks (GNNs) [7, 30, 31] have attracted a thrust of attention [16] for extending standard NNs to learn or infer over graph-structured data through the iterative message passing processes between nodes and their neighbors.

Link prediction is an important problem in graph-structured data analysis that predicts whether two nodes in a graph are likely to be linked [22]. It has a wide range of applications, for instance, the recommendation of hyperlinks of web pages [25], the reconstruction of metabolic network [23], the citations of academic papers [32], and the friend recommendations in Twitter and Facebook. Graph convolutional networks (GCNs)-based graph auto-encoders (GAEs) [15, 36] and variational graph auto-encoders (VGAEs) [15] are two typical unsupervised node embedding approaches to link prediction on graph-structure data. Compared to popular DNNs such as convolutional neural networks (CNNs) [20] and ResNet [10], GAEs, VGAEs, and their variants [8, 24] come with quite shallow architectures, often one or two layers. Recently, [29] has pointed out the reason for their using shallow structures is because linear cases (i.e., one-layer versions) of GAEs and VGAEs have already achieved good performance and often outperform their multi-layer versions, including two- or three-layer GCNs-based GAEs and VGAEs, on link prediction. Indeed, our experiments on real data also demonstrate that directly increasing the depth of GAEs and VGAEs does not improve link prediction performance, but rather decreases it; see Figures 1 and 5 (a). Considering the potential of DNNs with many layers in various applications, the ability of these current shallow GAEs- and VGAEs-based models to extract information from higher-order neighborhoods and node features is still limited.

Recently, a similar issue has also been observed in the (semi-) supervised learning with GNNs. For example, different models for node classification, such as GCN [16],

*Contact: qiang.cheng@uky.edu

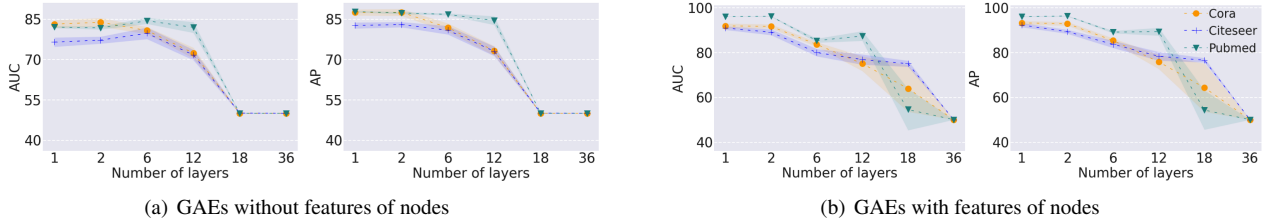


Figure 1. The link prediction results, including the area under the receiver operating characteristic (ROC) curves (AUC) and the average precision (AP) metric, of standard GCN-based GAEs with different numbers of layers ($k = 1, 2, 6, 12, 18,$ and 36). The results were averaged over 10 runs of 10 different random splits of datasets. The horizontal axis denotes the number of layers, and it is observed that the performance of GAEs degrades with the increase of layers.

GAT [35], and EGNN [6], usually achieved their best performance with two-layer structures. When stacking more layers and adopting non-linearity, the performance of these models tends to degrade. Such a phenomenon has been referred to as over-smoothing where, as the number of layers increases, the node representation in these models tends to converge to a certain value and thus become indistinguishable. Lately, a number of studies have been conducted to address the over-smoothing problem of (semi-) supervised learning with GNNs, for example, [2, 16, 21, 27, 39].

In general, GNNs-based node classification, such as [16], is (semi-) supervised learning, and its final output is a multi-dimensional vector, consisting of predicted labels for unlabeled nodes. In contrast, link prediction, such as [15], typically is regarded as an unsupervised learning task and its final output is an adjacency matrix which is much higher dimensional than the number of nodes. Thus, link prediction can be regarded as an inverse problem of decoding a noisy adjacency matrix with potentially many missing values of a graph into the underlying true values and thus appears to be more challenging than node classification in terms of supervision and potential output dimensionality. Besides, although the performance of both node classification and link prediction decreases with the increase of the number of layers, due to the nature of GNNs, the accuracies of node classification eventually converge to different constants [2, 37], while the final results of link prediction will converge to about 0.5 (see Figure 1). Given all these patent differences, while the recent development, such as [2, 39], makes deeper extension of GCN for node classification feasible, whether there is an advantage of increasing the depth of GAEs and VGAEs for link prediction still remains unclear.

In this paper, we study the deep extension of current GAEs and VGAEs for link prediction and respectively extend them into two deep models, DGAE and DVGA. To this end, the multi-scale information of seamlessly integrated adjacency matrix and node features will be effectively utilized. Specifically, we create an approach to exploit the multi-scale information by constructing residual

connections from the low-dimensional representations of the coherently combined adjacency matrix and node features of the graph. Because the low-fidelity input graph consists of noisy, missing connections and the node features may also contain useless or irrelevant features, the input graph is intrinsically low-dimensional in both graph structure and node features. To capture such an essential, low-dimensional structure and provision it at different scales, we generate the co-embeddings of the integrated adjacency matrix and node features by leveraging standard one-layer auto-encoders (AEs), and use them to produce multi-scale information via skipping connections, thereby further yielding the compact joint edge-node representation. To prevent the model from overfitting when going unnecessarily complex, we adopt helpful regularizations in our deep models. The contributions of the paper are summarized as follows:

- It effectively extends the shallow GAEs and VGAEs into two deep models, DGAE and DVGA. To our best knowledge, it is the first deep GAE- and VGAE-based models for link prediction.
- It innovatively incorporates standard AEs and graph AEs into a unified model. Standard AEs are leveraged to obtain the low-dimensional representation of the seamlessly integrated adjacency matrix and node features, forming the basis for constructing effective skip connections in graph AEs to extract multi-scale edge-node information jointly. Further, all the combination coefficients in our models are made trainable.
- Empirical experiments show that our proposed DGAE and DVGA models achieve competitive performance over current shallow GAEs, VGAEs, and their variants on link prediction consistently across benchmarking datasets.
- Theoretical results show that our deep extensions can inclusively express multiple polynomial filters with different orders.

The notations are given as follows. Let $G = (\mathbf{V}, \mathbf{E}, \mathbf{X})$ be an undirected graph, where \mathbf{V} and \mathbf{E} respectively denote the sets of nodes and edges, and $\mathbf{X} \in \mathbb{R}^{n \times m}$ is the node feature matrix. $\mathbf{A} \in \{0, 1\}^{n \times n}$ is the adjacency matrix associated with G . Here, n is the number of nodes, and m is the number of node features. $\|\cdot\|_{\mathbb{F}}^2$ denotes the Frobenius norm, and $\mathbb{E}[\cdot]$ is for the mathematical expectation.

The remainder of the paper is organized as follows. Firstly, it discusses the related work, then presents the proposed deep extensions, followed by extensive experiments and discussions. Finally, Section 6 concludes this paper.

2. Related Work

In this section, we briefly review the relevant studies in deepening models for GCNs [16]; then, we discuss the developments of link prediction based on GAEs and VGAEs.

2.1. Deepening GCNs for Node Classification

The deep extension of standard NNs greatly improves their learning performance, leading to a quantum leap in artificial intelligence and applications. For GCNs, the over-smoothing phenomenon, where the performance of GCNs degrades with the increase of number of layers, impedes the development of deep extensions of GCNs. Currently, two major types of efforts have been taken to gain deeper GCNs: The first type uses the residual connection [10], now a standard, proven-effective technique for training DNNs. For example, [16] used residual connections between hidden layers; [39] introduced the first deep GCN, JKNet, which concatenated the node representations in all previous layers. Although highly effective for DNNs over regular data, [16, 39] showed that adding residual connections in GCNs only mitigates the performance degradation as the network depth increases, while the resulting best performance is still dominated by shallow GCN models. Recently, [2] proposed a model, called GCNII, which combined a skipping connection from the input node features, to each layer and adopted the identity mapping as a regularization. GCNII showed good performance on node classification with deepened GCNs. The second type uses deep propagation to capture higher-order information in graph-structured data. However, this type of models [17, 38] are usually linear combinations of neighbor information in different layers, so in nature they are still regarded as shallow models [2].

Besides the techniques focusing on architectures, two main regularizations are usually adopted in deepening GCNs: 1) Identity mapping [9]. For example, [2] added an identity matrix to the weights of different layers of GCNII for regularization. 2) Dropout [13]. As a standard regularization technique in DNNs, it was also used for mitigating the effects of over-smoothing in GCNs. For instance, [27] randomly dropped out edges of the input graph to decel-

erate the performance degradation in deep GCNs for node classification.

In this paper, noticing the effectiveness of the residual connection on deepening DNNs over Euclidean data and GCNs for node classification, we will leverage the residual connection to deepen GAEs- and VGAEs-based models for link prediction; besides, we will also consider the above-mentioned regularizations in our proposed DGAE and DVGA. It is worthwhile to note that GAEs- and VGAEs-based link prediction is patently different from GCNs-based node classification. The former, as an unsupervised learning technique, mainly reconstructs the underlying true graph based on a low-fidelity version of the graph structure and node features with potentially many missing edges, and its final output is a full $n \times n$ matrix; in contrast, GCNs are (semi-) supervised learning models, which finally output an n -dimensional vector for labeling nodes. Therefore, deepening GAEs and VGAEs models for link prediction appears to be more challenging than deepening GCNs for node classification in terms of the availability of supervision information and potential output dimensions.

2.2. GAEs- and VGAEs-based Link Prediction

GAEs- and VGAEs-based link prediction is to encode the node features and the given noisy topological structure with potentially missing edges in a graph into a latent representation and then predict the likelihood of an association between all pairs of nodes.

Two-layer GAEs and VGAEs for link prediction were firstly proposed [15], which led to a series of subsequent developments of graph representations. By incorporating an adversarial training module, [24] introduced two variants, adversarially regularized graph auto-encoders (ARGAs) and adversarially regularized variational graph auto-encoders (ARVGAs), both of them required the matching of the underlying representation with a specific prior distribution while minimizing the reconstruction error of the graph structure. [8] revised the decoder in GAEs and VGAEs with an iterative graph refinement strategy, resulting in Graphite-AEs and Graphite-VAEs. In a recent study, [29] pointed out that linear cases of GAEs and VGAEs already achieved good performance compared to multi-layer cases, such as two- and three-layer GCNs-based GAEs and VGAEs, on link prediction. This study also questioned the relevance of using three citation network datasets, including Cora, Cite-seer, and Pubmed, to compare complex GAEs and VGAEs. The architectures of these models are usually not sufficiently deep; for example, in [24], a two-layer encoder was employed with a two-layer discriminator; in [8], a two-layer encoder and a three-layer decoder were combined with reverse message passing; in [29], one-layer, two-layer, and three-layer GAEs and VGAEs were analyzed.

For simplicity, this paper will focus on extending the

original GAEs and VGAEs; that is, our deepening is mainly for the encoder while retaining the original inner product architecture of the decoder. We will compare our deepened models with the shallow GAEs, VGAEs, and their variations as above-mentioned. Besides, we will also compare with Spectral Clustering (SC) [33] and DeepWalk [26] as two baselines for link prediction.

3. Proposed Model

In this section, we will present our first deep extension, DGAEs. Then, in Section 4 and Supplementary Materials, we will further discuss another similar extension, DVGAs.

3.1. An Attempt to Directly Deepen GAEs

GAE consists of an encoder and a decoder, and it utilizes low-fidelity topological structure information encoded in \mathbf{A} , which may be noisy with potentially many missing entries, and \mathbf{X} as a combined input to obtain a latent representation \mathbf{Z} , and then use the decoder to reconstruct an estimated $\hat{\mathbf{A}}$ from \mathbf{Z} . Because the adjacency matrix of the graph represents the similarity or association between the pairs of nodes, the decoder for link prediction usually adopts an inner product of the learned latent representation, $\langle \mathbf{Z}, \mathbf{Z}^T \rangle$. For later discussion, firstly we formalize the definition of a deepened k -layer GAE as follows:

$$\hat{\mathbf{A}} = \sigma(\langle \mathbf{Z}, \mathbf{Z}^T \rangle), \quad \mathbf{Z} = \tilde{\mathbf{A}} f_{k-1}(\cdots \tilde{\mathbf{A}} f_1(\tilde{\mathbf{A}} \mathbf{X})) \mathbf{W}_k, \quad (1)$$

where $\hat{\mathbf{A}}$ is a reconstructed adjacency matrix as the output of link prediction, $\mathbf{Z} \in \mathbb{R}^{n \times h}$, h is the dimension of the latent representation, $\sigma(\cdot)$ is a sigmoid function, and $\tilde{\mathbf{A}} = \mathbf{D}^{-\frac{1}{2}}(\mathbf{A} + \mathbf{I})\mathbf{D}^{-\frac{1}{2}}$. Here, \mathbf{D} is a diagonal matrix with $\mathbf{D}_{ii} = \sum_j (\mathbf{A} + \mathbf{I})_{ij}$, and \mathbf{I} is the identity matrix. In this paper, other than the output layer, we adopt ReLU as activation functions. Thus, we have $f_i(\tilde{\mathbf{A}} \mathbf{X}) = \text{ReLU}(\tilde{\mathbf{A}} \mathbf{X} \mathbf{W}_i)$, $i \geq 1$. For $i = 0$, we take $f_0(\tilde{\mathbf{A}} \mathbf{X}) = \tilde{\mathbf{A}} \mathbf{X} \mathbf{W}_1$. It is clear that we have the following special cases: When $k = 1$ and 3, (1) respectively reduces to the linear and three-layer cases [29]; when $k = 2$, (1) becomes GAE [16].

For model (1), we train it by optimizing the following reconstruction error as a cost function between the input \mathbf{A} and the reconstructed $\hat{\mathbf{A}}$, which was also used in [16]:

$$\mathcal{L}_1 = \mathbb{E}_{\mathbf{Z}} [\log \sigma(\langle \mathbf{Z}, \mathbf{Z}^T \rangle)]. \quad (2)$$

For k -layer GAE, we compute the cases of $k = 1$ (linear case), 2 (GAE), 6, 12, 18, and 36 over three standard datasets, with the results shown in Figure 1. It is seen that the performance of link prediction, in AUC and AP, decreases with the increase of depth. Interestingly, it is observed that on all three datasets, when the number of layers reaches 36, all the results converge to about 0.5. With $\hat{\mathbf{A}} = \mathbf{D}^{-\frac{1}{2}}(\mathbf{A} + \mathbf{I})\mathbf{D}^{-\frac{1}{2}}$, the GAE model corresponds to a

lazy random walk, where at each time step the walker either stays at the current node or walks to a random neighbor, each with a probability of 0.5. Thus, the link prediction with GAE will finally converge to 0.5 with the increase of layers.

3.2. Skip Connection of Node Features

In Figure 1, it is noted that the good performance is generally achieved by models with one and two layers, implying that the information from the shallow layers will play an important role in the final performance. In the development of deepened GCNs for node classification, residual connections are used to retain the information in the previous layers; for example, [2] added the input node features or the output of a fully connected neural network on node features to each layer. For link prediction, the (potentially high-dimensional) node features may contain irrelevant features and usually are noisy. Inspired by the observation obtained from Figure 1, we propose to capture the essential, low-dimensional subspace of the input node features. Thus, we propose to incorporate standard AEs on node features to obtain latent low-dimensional representations at different layers and combine them using skip connections in (1), thereby maximally preserving the useful node information in previous layers:

$$\begin{cases} \hat{\mathbf{A}} = \sigma(\langle \mathbf{Z}, \mathbf{Z}^T \rangle), \\ \mathbf{Z} = \alpha_{k-1} \tilde{\mathbf{A}} f_{k-1}(\cdots \tilde{\mathbf{A}} (\alpha_1 f_1(\tilde{\mathbf{A}} \mathbf{X}) + (1 - \alpha_1) g_1(\mathbf{X}))) \\ \quad \mathbf{W}_k + (1 - \alpha_{k-1}) \tilde{\mathbf{A}} g_{k-1}(\mathbf{X}) \mathbf{W}_k, \\ g'_i(g_i(\mathbf{X})) = \mathbf{X}, i = 1, 2, \dots, k - 1, \end{cases} \quad (3)$$

where g_i and g'_i are respectively the encoder and decoder of standard AEs, the dimensions of g'_i and f_i are required to be the same, and $0 \leq \alpha_i \leq 1$ ($i = 1, 2, \dots, k - 1$) are combination coefficients.

For optimizing (3), we minimize the following combined reconstruction errors:

$$\mathcal{L}_2 = \sum_{i=1}^{k-1} \lambda_i \|g'_i(g_i(\mathbf{X})) - \mathbf{X}\|_{\mathbb{F}}^2 + \lambda_0 \mathcal{L}_1, \quad (4)$$

where $\lambda_i \geq 0$ ($i = 0, 1, \dots, k - 1$) are hyper-parameters balancing the reconstruction errors of standard AEs with graph AEs.

For model (3), we compute the cases of $k = 6, 12, 18$, and 36, and compare the results with those obtained using k -layer GAEs in Figure 2. It is found that (3) can effectively avoid the performance degradation when increasing the number of layers in (1); in particular, the improvement over Citeseer is substantial. Further, the standard deviations for (3) are much smaller than the GAE counterpart.

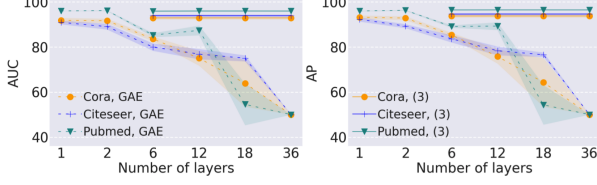


Figure 2. The comparison of model (3) with k -layer GAEs (1). The results were averaged over 10 runs of 10 different random splits of datasets. The horizontal axis denotes the number of layers. For $k = 1, 2$, the results for (3) and k -layer GAEs are essentially the same (and thus not depicted for (3) for visual clarity).

3.3. Integrating Adjacency Information and Node Features

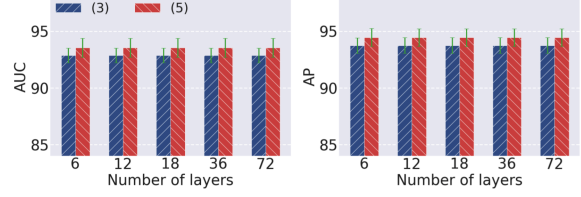
Model (3) can exploit the low-rank subspace of potentially high-dimensional yet noisy node features, which may be sufficient for deepening the GCNs for node classification. However, the final output of link prediction is directly related to adjacency information; thus, predicting links in GAEs is different from the node labelling process for node classification in GCNs. In particular, the intrinsic structure of the low-fidelity input adjacency matrix is still underutilized in model (3). This input matrix is usually noisy with potentially many missing values; yet, usually it also resides on an essential, low-rank subspace due to the clustering structure of connected nodes [4]. To exploit such a low-rank subspace, we propose to co-embed the node features and the input adjacency matrix. Specifically, we further enhance model (3) using the combination of adjacency information and node features as input to standard AEs as follows:

$$\begin{cases} \hat{\mathbf{A}} = \sigma(\langle \mathbf{Z}, \mathbf{Z}^T \rangle), \\ \mathbf{Z} = \alpha_{k-1} \tilde{\mathbf{A}} f_{k-1}(\cdots \tilde{\mathbf{A}}(\alpha_1 f_1(\tilde{\mathbf{A}} \mathbf{X}) + (1 - \alpha_1) \\ g_1(\tilde{\mathbf{A}} \mathbf{X}))) \mathbf{W}_k + (1 - \alpha_{k-1}) \tilde{\mathbf{A}} g_{k-1}(\tilde{\mathbf{A}} \mathbf{X}) \mathbf{W}_k, \\ g'_i(g_i(\tilde{\mathbf{A}} \mathbf{X})) = \tilde{\mathbf{A}} \mathbf{X}, i = 1, 2, \dots, k-1, \end{cases} \quad (5)$$

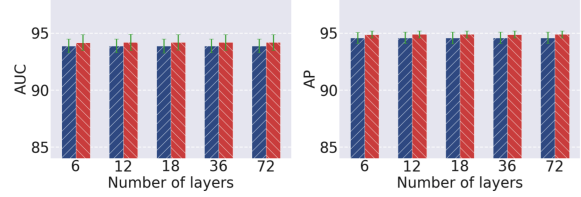
where the compact co-embedding is formed using standard AEs for nonlinearly capturing the low-rank subspace from the seamlessly integrated (convolved) adjacency matrix and node matrix. The co-embedding is then provided to various layers of our model via the dense skip connections. Correspondingly, we use the following cost function for optimization, which incorporates the reconstruction errors of using standard AEs for co-embedding:

$$\mathcal{L}_3 = \sum_{i=1}^{k-1} \lambda_i \|g'_i(g_i(\mathbf{A} \mathbf{X})) - \mathbf{A} \mathbf{X}\|_F^2 + \lambda_0 \mathcal{L}_1. \quad (6)$$

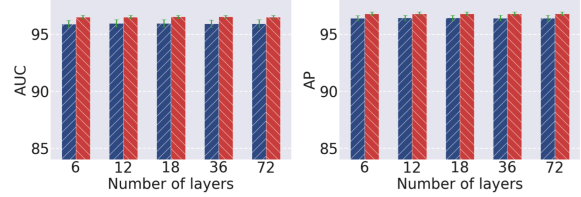
We empirically compare the model in (5) with that in (3) for $k = 6, 12, 18, 36$, and 72; see Figure 3. It is evident



(a) Cora



(b) Citeseer



(c) Pubmed

Figure 3. The comparison of the models in (5) and (3) on Cora, Citeseer, and Pubmed. The results are averaged over 10 runs of 10 different random splits of datasets. The horizontal axis denotes the number of layers.

that model (5) has better performance than model (3) on Cora, Citeseer, and Pubmed, demonstrating that capturing the low-rank subspace of the seamlessly integrated graph structure with node features and using it as input to various layers via the residual connections in GAEs is conducive to the final link prediction.

3.4. Deep Model with Regularization

Noting that the identity matrix [9] was helpful in GCNII [2] for node classification as a regularization, we consider adding it as a regularization term in (5) to potentially boost the performance. The change is mainly for the \mathbf{Z} quantity in (5), and the modified version is as follows:

$$\begin{aligned} \mathbf{Z} = & \alpha_{k-1} \tilde{\mathbf{A}} f'_{k-1}(\cdots \tilde{\mathbf{A}}(\alpha_1 f'_1(\tilde{\mathbf{A}} \mathbf{X}) + (1 - \alpha_1) \\ & g_1(\tilde{\mathbf{A}} \mathbf{X}))) ((1 - \beta_k) \mathbf{W}_k + \beta_k \mathbf{I}_k) \\ & + (1 - \alpha_{k-1}) \tilde{\mathbf{A}} g_{k-1}(\tilde{\mathbf{A}} \mathbf{X}) ((1 - \beta_k) \mathbf{W}_k + \beta_k \mathbf{I}_k), \end{aligned} \quad (7)$$

where $f'_i(\tilde{\mathbf{A}} \mathbf{X}) = \text{ReLU}(\tilde{\mathbf{A}} \mathbf{X}((1 - \beta_i) \mathbf{W}_i + \beta_i \mathbf{I}_i))$, and \mathbf{I}_i is the identity matrix, $i = 1, 2, \dots, k-1$. Besides, $0 \leq \alpha_i \leq 1$ ($i = 1, 2, \dots, k-1$) and $0 \leq \beta_i \leq 1$ ($i = 1, 2, \dots, k$) are combination coefficients.

4. Experiments

In this section, we will perform experiments to extensively verify our deep extensions by comparing them with shallow models and contemporary GAEs- and VGAEs-based link prediction models on many benchmarking datasets.

4.1. Datasets to Be Used

Firstly we compare three standard benchmark datasets, including Cora, Citeseer, and Pubmed [32], which are widely used in GNNs. For further validating the performance of our deep extensions, we use other three datasets: Chameleon [28], Texas, and Wisconsin [25]. We summarize the statistics of these datasets in Table 1.

| DATASET | # NODES | # EDGES | # FEATURES |
|-----------|---------|---------|------------|
| CORA | 2,708 | 5,429 | 1,433 |
| CITSEER | 3,327 | 4,732 | 3,703 |
| PUBMED | 19,717 | 44,338 | 500 |
| CHAMELEON | 2,277 | 36,101 | 2,325 |
| TEXAS | 183 | 309 | 1,703 |
| WISCONSIN | 251 | 499 | 1,703 |

Table 1. Statistics of datasets.

4.2. Evaluation Metrics

We evaluate performance based on two metrics, AUC and AP, which are also adopted for link prediction in [15, 8, 24]. For all experiments, the obtained mean results and standard deviations are for 10 runs over 10 different random train/validation/test splits of datasets.

4.3. Parameter/Experiment Settings

In all experiments, for our deep extension, we set the maximum number of epochs to be 200, and we adopt the Adam optimizer [14] with an initial learning rate of 0.01. We follow the training scheme in [15, 24]: for the links of all datasets, we randomly split them into training, validation, and testing sets by a ratio of 85 : 5 : 10; we train all the models by removing 15% of links while keeping node features, and the validation and testing sets are from the removed edges and the corresponding node pairs; the weights of models are initialized by using the Glorot uniform technique [5]. In addition, we perform a grid search to tune hyper-parameters for our different depth models according to the performance on the validation set, and the details of these hyper-parameter are given in the Supplementary Materials. For simplicity, in the following experiments we construct our deep encoders with $(k - 1)$ 32-neuron hidden layers and a 16-neuron latent embedding layer, and we denote the model in (5) as $DGAE_\alpha$.

For baselines SC, DeepWalk, 2-layer GAE, and 2-layer VGAE, we follow the settings in [15]; for the rest of base-

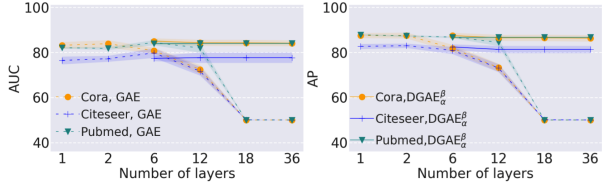


Figure 4. The comparison of GAEs with $DGAE_\alpha^\beta$ without using node features. The results are on Cora, Citeseer, and Pubmed. With the number of layers $k = 1, 2$, GAEs and $DGAE_\alpha^\beta$ have essentially the same results (and thus only GAEs are depicted).

lines, linear GAE, linear VGAE [29], ARG, ARVGA [24], Graphite-AE, and Graphite-VAE [8], we follow the settings described in their corresponding papers.

4.4. Results on Cora, Citeseer, and Pubmed

We summarize the AUC and AP results (mean±standard deviation) of our experiments in Table 2¹. Both 6-layer and 36-layer $DGAE_\alpha$ architectures achieve competitive results; in particular, our $DGAE_\alpha$ achieves consistently better predictive performance than the methods in comparison.

We denote the model in (7) as $DGAE_\alpha^\beta$, and we compare it with $DGAE_\alpha$ in Figure 1 in the Supplementary Materials. It is observed that $DGAE_\alpha^\beta$ achieves relatively better performance.

Also, we study the performance of $DGAE_\alpha$ using the dropout, and the analysis is given in Figure 2 in the Supplementary Material. It is seen that the effect of dropout on $DGAE_\alpha$ is quite limited.

4.5. Variants

In this section, we will discuss two variants of $DGAE_\alpha^\beta$.

4.5.1 Without Node Features

Now, we consider the case without using the node features for link prediction; that is, we set \mathbf{X} in $DGAE_\alpha^\beta$ to be the identity matrix, and then we compare this node-featureless $DGAE_\alpha^\beta$ with the node-featureless version of GAE. We summarize the results in Figure 4, and our featureless $DGAE_\alpha^\beta$ keeps competitive performance with the increase of layers.

4.5.2 Variational Case

Next, we present a deep extension of VGAE, called $DVGA_\alpha^\beta$, where \mathbf{Z} is not directly generated by the encoder of DGAEs, but rather a Gaussian distribution. More details

¹Here, we illustrate the results for $DGAE_\alpha$ with 6, 36, and 72 layers; the results with other numbers of layers can be observed in Figure 3.

| DATASET | CORA | | CITSEER | | PUBMED | |
|----------------------|---------------------|---------------------|---------------------|---------------------|---------------------|---------------------|
| | AUC (%) | AP (%) | AUC (%) | AP (%) | AUC (%) | AP (%) |
| SC | 85.36 ± 1.62 | 88.41 ± 1.18 | 77.26 ± 1.87 | 80.24 ± 1.36 | 80.16 ± 0.54 | 79.89 ± 0.66 |
| DEEPWALK | 76.41 ± 1.70 | 81.78 ± 1.02 | 64.15 ± 1.81 | 74.60 ± 1.21 | 73.32 ± 0.60 | 81.53 ± 0.40 |
| ARGA | 92.10 ± 1.18 | 93.25 ± 0.93 | 90.43 ± 0.73 | 92.04 ± 0.83 | 95.55 ± 0.21 | 95.76 ± 0.19 |
| GRAPHITE-AE | 91.29 ± 0.83 | 92.63 ± 0.70 | 88.84 ± 1.62 | 89.64 ± 1.60 | 96.24 ± 0.23 | 96.42 ± 0.21 |
| LINEAR-GAE | 91.86 ± 1.06 | 93.20 ± 0.80 | 90.89 ± 0.79 | 92.24 ± 0.95 | 96.01 ± 0.06 | 95.98 ± 0.11 |
| 2-GAE | 91.61 ± 0.92 | 92.81 ± 0.82 | 89.04 ± 1.27 | 89.26 ± 0.87 | 96.13 ± 0.14 | 96.26 ± 0.17 |
| 6-GAE | 83.58 ± 1.01 | 85.32 ± 0.97 | 79.95 ± 1.64 | 83.63 ± 1.59 | 85.27 ± 0.86 | 89.10 ± 0.54 |
| 36-GAE | 50.00 ± 0.00 | 50.00 ± 0.00 | 50.00 ± 0.00 | 50.00 ± 0.00 | 50.00 ± 0.00 | 50.00 ± 0.00 |
| 72-GAE | 50.00 ± 0.00 | 50.00 ± 0.00 | 50.00 ± 0.00 | 50.00 ± 0.00 | 50.00 ± 0.00 | 50.00 ± 0.00 |
| 6-DGAE _α | 93.55 ± 0.84 | 94.46 ± 0.78 | 94.16 ± 0.69 | 94.86 ± 0.30 | 96.51 ± 0.16 | 96.79 ± 0.15 |
| 36-DGAE _α | 93.54 ± 0.84 | 94.45 ± 0.78 | 94.17 ± 0.68 | 94.87 ± 0.30 | 96.52 ± 0.15 | 96.79 ± 0.16 |
| 72-DGAE _α | 93.53 ± 0.85 | 94.45 ± 0.78 | 94.17 ± 0.69 | 94.88 ± 0.29 | 96.51 ± 0.16 | 96.79 ± 0.17 |

Table 2. AUC (%) and AP (%) scores for different algorithms on link prediction.

about k -layer VGAE and DVGA_α^β are provided in the Supplementary Material.

Firstly we compare DVGA_α^β with VGAE and its variants by using different numbers of layers, and then we further perform the comparisons of 6-layer DVGA_α^β with linear VGAE, 2-layer VGAE, 6-layer VGAE, ARVGA, and Graphite-VAE; see Figure 5. It is clear that DVGA_α^β with only 6 layers already has a patent advantage over other variational algorithms.

4.6. Validation on More Datasets

While [29] questioned the possibility of further improvement of using the three standard network datasets, Cora, Citeseer, and Pubmed, our deep extensions demonstrate clear competitive performance over current state-of-the-art algorithms on these datasets; see Table 2. For further verifying the performance of our deep extensions, we evaluate DGAE_α^β on three more datasets; the results are summarized in Table 3. It is seen that our deep extensions achieve superior performance to almost all algorithms in comparison.

5. Discussions

In this section, we provide discussions and further analysis of our proposed deep extensions.

5.1. Combination of Standard and Graph AEs

The combining of standard AEs in (3) and (5) may seem similar to the layer-wise pre-training technique in [1, 12], in that we train a series of shallow standard AEs to obtain multiple low-dimensional representations in an unsupervised fashion. But the essential difference exists: The shallow standard AEs in our model are independent, and the extracted latent representations are used for each new skip connection in the entire deep GAEs, which are combined integrally. In contrast, for the layer-wise pre-training, mul-

multiple standard AEs are stacked and each low-dimensional representation is only input to the next layer.

Moreover, from the results in Figure 3, it is evident that using standard AEs to jointly exploit the essential, low-rank subspace of the graph structure and node features for co-embedding is more conducive for the final link prediction than without.

5.2. Visualization

For understanding the difference between the learning in DGAE_α^β and GAEs, we visualize the low-dimensional graph embeddings learned by DGAE_α^β and GAEs with different numbers of layers using 2D t-SNE [34]. The 2D embedding results on Cora are visually presented in Figure 6. It is observed that DGAE_α^β leads to more separated graph embeddings than GAEs, which are in line with the our quantitative results in AUC and AP shown above.

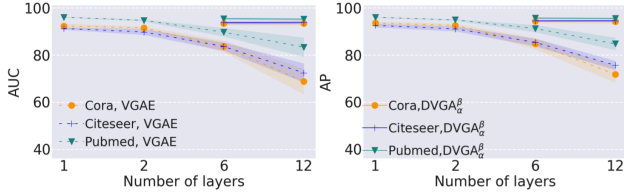
5.3. Multiple Graph AEs with Different Depths

Next, we further analyze why our deep extensions can stabilize and enhance link prediction. We theoretically show that our deep extensions inclusively express multiple polynomial filters with different orders.

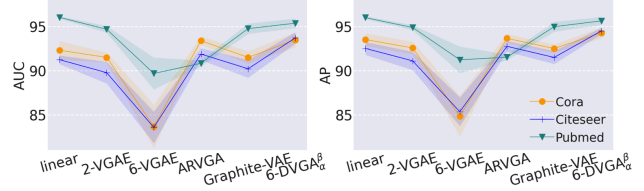
Theorem 1. *A k -layer ($k \geq 3$) DGAE_α is a linear combination of 2-order to k -order polynomial filters with arbitrary combination coefficients.*

Proof. We consider the case where all activation functions in (5) are linear. By Lemma 1 in the Supplementary Materials, Theorem 1 is easily proved. \square

Proposition 1. *1-layer DGAE_α is a linear GAE, and 2-layer DGAE_α is a linear combination of 2-order polynomial filters; in particular, 2-layer DGAE_α is a 2-layer GAE plus a linear GAE that takes a low-dimensional representation of the standard AE as input.*



(a) The comparison of $DVGA_{\alpha}^{\beta}$ with VGAEs by different numbers of layers. With $k = 1, 2$, VGAEs and $DVGA_{\alpha}^{\beta}$ have essentially the same results (and thus only VGAEs are depicted)



(b) The comparison of $DVGA_{\alpha}^{\beta}$ with other variational algorithms

Figure 5. The comparisons of variational models on Cora, Citeseer, and Pubmed.

| DATASET | CHAMELEON | | TEXAS | | WISCONSIN | |
|-----------------------------|---------------------|---------------------|---------------------|---------------------|----------------------|---------------------|
| | AUC (%) | AP (%) | AUC (%) | AP (%) | AUC (%) | AP (%) |
| LINEAR-GAE | 45.21 ± 3.75 | 53.74 ± 3.79 | 12.97 ± 11.78 | 40.41 ± 8.45 | 21.98 ± 7.24 | 44.53 ± 5.64 |
| 2-GAE | 46.33 ± 6.26 | 54.62 ± 5.77 | 22.19 ± 12.65 | 46.35 ± 8.55 | 34.63 ± 11.13 | 57.09 ± 7.12 |
| 6-GAE | 37.67 ± 5.80 | 49.71 ± 4.69 | 15.31 ± 10.66 | 42.38 ± 8.73 | 19.51 ± 7.88 | 45.14 ± 8.00 |
| 36-GAE | 50.00 ± 0.00 | 50.00 ± 0.00 | 50.00 ± 0.00 | 50.00 ± 0.00 | 50.00 ± 0.00 | 50.00 ± 0.00 |
| 72-GAE | 50.00 ± 0.00 | 50.00 ± 0.00 | 50.00 ± 0.00 | 50.00 ± 0.00 | 50.00 ± 0.00 | 50.00 ± 0.00 |
| 6-DGAE $_{\alpha}^{\beta}$ | 56.89 ± 4.14 | 62.89 ± 4.42 | 45.78 ± 9.63 | 61.06 ± 8.74 | 53.95 ± 10.92 | 67.76 ± 8.62 |
| 36-DGAE $_{\alpha}^{\beta}$ | 58.35 ± 6.61 | 60.60 ± 5.78 | 45.16 ± 10.86 | 60.44 ± 9.74 | 54.20 ± 10.55 | 67.78 ± 8.73 |
| 72-DGAE $_{\alpha}^{\beta}$ | 62.26 ± 0.17 | 65.02 ± 1.46 | 46.09 ± 9.56 | 61.04 ± 8.82 | 53.70 ± 9.52 | 67.46 ± 7.80 |

Table 3. AUC (%) and AP (%) scores for k -GAEs with $k = 1, 2, 6, 36, 72$, and $DGAE_{\alpha}^{\beta}$ with layers 6, 36, and 72.

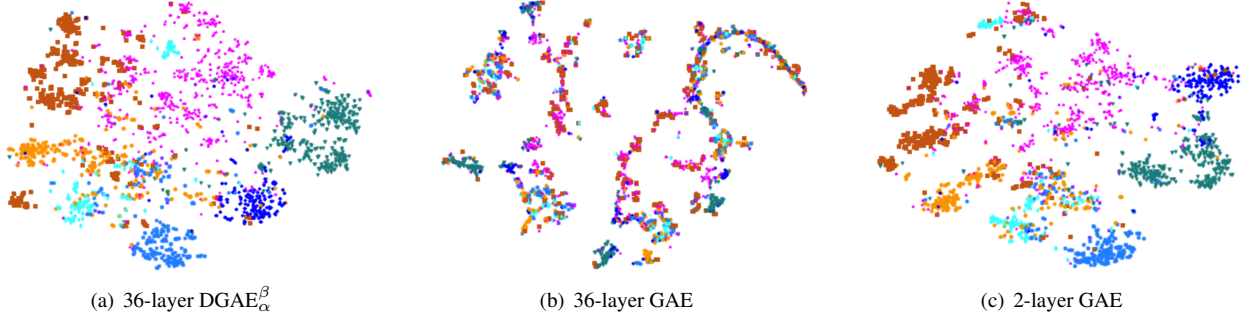


Figure 6. The visualization of low-dimensional embeddings for Cora. Each color denotes a document class. During training, both $DGAE_{\alpha}^{\beta}$ and GAE do not need to access class information.

Proof. Let $f_0(\tilde{\mathbf{A}}\mathbf{X}) = \tilde{\mathbf{A}}\mathbf{X}\mathbf{W}_1$, then it is obvious that, for $k = 1$, (5) reduces to the linear case. For $k = 2$, (5) can be written as

$$\begin{aligned} & \alpha_1 \tilde{\mathbf{A}}^2 \mathbf{X} \mathbf{W}_1 \mathbf{W}_2 + (1 - \alpha_1) \tilde{\mathbf{A}} g_1(\tilde{\mathbf{A}}\mathbf{X}) \mathbf{W}_2 \\ &= \alpha_1 \tilde{\mathbf{A}}^2 \mathbf{X} \mathbf{W}_1 \mathbf{W}_2 + (1 - \alpha_1) \tilde{\mathbf{A}}^2 \mathbf{X} \mathbf{W}_1^g \mathbf{W}_2 \end{aligned} \quad (8)$$

where $\tilde{\mathbf{A}}\mathbf{X}\mathbf{W}_1^g = g_1(\tilde{\mathbf{A}}\mathbf{X})$. So, Proposition 1 is proved. \square

Therefore, our deep extensions essentially imply multiple (variational) GAEs with different depths. In practical implementation, the combination coefficients in our models are all trainable, thereby making our extensions straightforward to train.

6. Conclusion

Link prediction using GAEs- or VGAEs-based models encodes the graph structure and node features into a low-dimensional embedding, and then adopts a decoder to reconstruct the graph in the original space to infer the potential links. In this paper, we aim to overcome the limitation of current state-of-the-art methods that can only use shallow GAEs and VGAEs effectively. By seamlessly integrating the graph structure and node features and deeply combining standard AEs and graph AEs, we develop effective deep extensions for shallow GAEs and VGAEs on link prediction. Our innovative extension leverages the joint optimization of standard and graph AEs, and it also exploits a residual connection in graph AEs from the low-dimensional compact representation to the combination of adjacency information and node features in graph-structured data. Fur-

ther, we also take advantage of regularization techniques of using the identity matrix and dropout in our proposed models. Extensive experiments on various datasets empirically demonstrate the competitive performance of our deepened graph models on link prediction. In addition, although our current extension is for the encoder, whether it is applicable to deepen the decoder will be further investigated in our future work.

References

- [1] Yoshua Bengio, Pascal Lamblin, Dan Popovici, and Hugo Larochelle. Greedy layer-wise training of deep networks. In *Advances in Neural Information Processing Systems*, pages 153–160, Cambridge, Massachusetts, United States, December 2006. [7](#)
- [2] Ming Chen, Zhewei Wei, Zengfeng Huang, Bolin Ding, and Yaliang Li. Simple and deep graph convolutional networks. In *International Conference on Machine Learning*, pages 1725–1735, Vienna, Austria, July 2020. [2](#), [3](#), [4](#), [5](#)
- [3] Dan Ciregan, Ueli Meier, and Jürgen Schmidhuber. Multi-column deep neural networks for image classification. In *Conference on Computer Vision and Pattern Recognition*, pages 3642–3649, Providence, Rhode Island, United States, June 2012. [1](#)
- [4] Santo Fortunato. Community detection in graphs. *Physics Reports*, 486(3-5):75–174, February 2010. [5](#)
- [5] Xavier Glorot and Yoshua Bengio. Understanding the difficulty of training deep feedforward neural networks. In *International Conference on Artificial Intelligence and Statistics*, pages 249–256, Chia Laguna Resort, Sardinia, Italy., May 2010. [6](#)
- [6] Liyu Gong and Qiang Cheng. Exploiting edge features for graph neural networks. In *IEEE Conference on Computer Vision and Pattern Recognition*, pages 9211–9219, Long Beach, California, United States, June 2019. [2](#)
- [7] Marco Gori, Gabriele Monfardini, and Franco Scarselli. A new model for learning in graph domains. In *IEEE International Joint Conference on Neural Networks*, pages 729–734, Montreal, Québec, Canada, July-August 2005. [1](#)
- [8] Aditya Grover, Aaron Zweig, and Stefano Ermon. Graphite: Iterative generative modeling of graphs. In *International Conference on Machine Learning*, pages 2434–2444, Long Beach, California, United States, June 2019. [1](#), [3](#), [6](#)
- [9] Moritz Hardt and Tengyu Ma. Identity matters in deep learning. In *International Conference on Learning Representations*, Toulon, France, April 2017. [3](#), [5](#)
- [10] Kaiming He, Xiangyu Zhang, Shaoqing Ren, and Jian Sun. Deep residual learning for image recognition. In *IEEE Conference on Computer Vision and Pattern Recognition*, pages 770–778, Las Vegas, Nevada, United States, June 2016. [1](#), [3](#)
- [11] Geoffrey Hinton, Li Deng, Dong Yu, George E. Dahl, Abdel rahman Mohamed, Navdeep Jaitly, Andrew Senior, Vincent Vanhoucke, Patrick Nguyen, Tara N. Sainath, and Brian Kingsbury. Deep neural networks for acoustic modeling in speech recognition: The shared views of four research groups. *IEEE Signal Processing Magazine*, 29(6):82–97, November 2012. [1](#)
- [12] Geoffrey Everest Hinton and Ruslan R. Salakhutdinov. Reducing the dimensionality of data with neural networks. *Science*, 313(5786):504–507, July 2006. [7](#)
- [13] Geoffrey Everest Hinton, Nitish Srivastava, Alex Krizhevsky, Ilya Sutskever, and Ruslan R. Salakhutdinov. Improving neural networks by preventing co-adaptation of feature detectors. *arXiv:1207.0580*, <https://arxiv.org/abs/1207.0580>, July 2012. [3](#)
- [14] Diederik P. Kingma and Jimmy Lei Ba. Adam: a method for stochastic optimization. In *International Conference for Learning Representations*, San Diego, California, USA, May 2015. [6](#)
- [15] Thomas N. Kipf and Max Welling. Variational graph auto-encoders. *arXiv:1611.07308*, <https://arxiv.org/abs/1611.07308>, November 2016. [1](#), [2](#), [3](#), [6](#)
- [16] Thomas N. Kipf and Max Welling. Semi-supervised classification with graph convolutional networks. In *International Conference on Learning Representations*, Toulon, France, April 2017. [1](#), [2](#), [3](#), [4](#)
- [17] Johannes Klicpera, Stefan Weissenberger, and Stephan Günnemann. Diffusion improves graph learning. In *Advances in Neural Information Processing Systems*, pages 13354–13366, Vancouver, British Columbia, Canada, December 2019. [3](#)
- [18] Alex Krizhevsky, Ilya Sutskever, and Geoffrey E. Hinton. Imagenet classification with deep convolutional neural networks. In *Advances in Neural Information Processing Systems*, pages 1097–1105, Lake Tahoe, California, United States, December 2012. [1](#)
- [19] Quoc V. Le, Marc’Aurelio Ranzato, Rajat Monga, Matthieu Devin, Kai Chen, Greg S. Corrado, Jeff Dean, and Andrew Y. Ng. Building high-level features using large scale unsupervised learning. In *International Conference on Machine Learning*, pages 507–514, Edinburgh, Scotland, United Kingdom, June 2012. [1](#)
- [20] Yann LeCun, Léon Bottou, Yoshua Bengio, and Patrick Haffner. Gradient-based learning applied to document recognition. *Proceedings of the IEEE*, 86(11):2278–2324, November 1998. [1](#)
- [21] Qimai Li, Zhichao Han, and Xiao-Ming Wu. Deeper insights into graph convolutional networks for semi-supervised learning. In *AAAI Conference on Artificial Intelligence*, pages 3538–3545, New Orleans, Louisiana, United States, February 2018. [2](#)
- [22] David Liben-Nowell and Jon Kleinberg. The link-prediction problem for social networks. In *International Conference on Information and Knowledge Management*, pages 556–559, New Orleans, Louisiana, United States, November 2003. [1](#)
- [23] Tolutola Oyetunde, Muhan Zhang, Yixin Chen, Yinjie Tang, and Cynthia Lo. BoostGAPFILL: improving the fidelity of metabolic network reconstructions through integrated constraint and pattern-based methods. *Bioinformatics*, 33(4):608–611, February 2017. [1](#)
- [24] Shirui Pan, Ruiqi Hu, Guodong Long, Jing Jiang, Lina Yao, and Chengqi Zhang. Adversarially regularized graph autoencoder for graph embedding. In *International Joint Confer-*

- ence on Artificial Intelligence, pages 2609–2615, Stockholm, Sweden, July 2018. 1, 3, 6
- [25] Hongbin Pei, Bingzhe Wei, Kevin Chen-Chuan Chang, Yu Lei, and Bo Yang. Geom-gcn: Geometric graph convolutional networks. In *International Conference on Learning Representations*, Addis Ababa, Ethiopia, April 2020. 1, 6
- [26] Bryan Perozzi, Rami Al-Rfou, and Steven Sol Skiena. Deepwalk: Online learning of social representations. In *ACM SIGKDD international conference on Knowledge discovery and data mining*, pages 701–710, New York, New York, United States, August 2014. 4
- [27] Yu Rong, Wenbing Huang, Tingyang Xu, and Junzhou Huang. Dropedge: Towards deep graph convolutional networks on node classification. In *International Conference on Learning Representations*, Addis Ababa, Ethiopia, April 2020. 2, 3
- [28] Benedek Rozemberczki, Carl Allen, and Rik Sarkar. Multi-scale attributed node embedding. *arXiv:1909.13021*, <https://arxiv.org/abs/1909.13021>, March 2020. 6
- [29] Guillaume Salha, Romain Hennequin, and Michalis Vazirgiannis. Simple and effective graph autoencoders with one-hop linear model. In *European Conference on Machine Learning and Principles and Practice of Knowledge Discovery in Databases*, Ghent, Belgium, September 2020. 1, 3, 4, 6, 7
- [30] Franco Scarselli, Marco Gori, Ah Chung Tsoi, Markus Hagenbuchner, and Gabriele Monfardini. The graph neural network model. *IEEE Transactions on Neural Networks*, 20(1):61–80, January 2009. 1
- [31] Franco Scarselli, Ah Chung Tsoi, Marco Gori, and Markus Hagenbuchner. Graphical-based learning environments for pattern recognition. In *Joint IAPR International Workshops on Statistical Techniques in Pattern Recognition and Structural and Syntactic Pattern Recognition*, pages 42–56, Lisbon, Portugal, August 2004. 1
- [32] Prithviraj Sen, Galileo Namata, Mustafa Bilgic, Lise Getoor, Brian Gallagher, and Tina Eliassi-Rad. Collective classification in network data. *AI Magazine*, 29(3):93–106, September 2008. 1, 6
- [33] Lei Tang and Huan Liu. Leveraging social media networks for classification. *Data Mining and Knowledge Discovery*, 23(3):447–478, January 2011. 4
- [34] Laurens van der Maaten and Geoffrey Hinton. Visualizing data using t-SNE. *Journal of Machine Learning Research*, 9(11):2579–2605, November 2008. 7
- [35] Petar Veličković, Guillem Cucurull, Arantxa Casanova, Adriana Romero, Pietro Liò, and Yoshua Bengio. Graph attention networks. In *International Conference on Learning Representations*, Vancouver, British Columbia, Canada, April-May 2018. 2
- [36] Daixin Wang, Peng Cui, and Wenwu Zhu. Structural deep network embedding. In *ACM SIGKDD International Conference on Knowledge Discovery and Data Mining*, pages 1225–1234, San Francisco, California, United States, August 2016. 1
- [37] Guangtao Wang, Rex Ying, Jing Huang, and Jure Leskovec. Improving graph attention networks with large margin-based constraints. *arXiv:1910.11945*, <https://arxiv.org/abs/1910.11945>, October 2019. 2
- [38] Felix Wu, Amauri Souza, Tianyi Zhang, Christopher Fifty, Tao Yu, and Kilian Weinberger. Simplifying graph convolutional networks. In *International Conference on Machine Learning*, pages 6861–6871, Long Beach, California, United States, June 2019. 3
- [39] Keyulu Xu, Chengtao Li, Yonglong Tian, Tomohiro Sonobe, Ken ichi Kawarabayashi, and Stefanie Jegelka. Representation learning on graphs with jumping knowledge networks. In *International Conference on Machine Learning*, pages 5453–5462, Stockholm, Sweden, July 2018. 2, 3